EXTENDED TARGET FREQUENCY RESPONSE ESTIMATION USING INFINITE HMM IN COGNITIVE RADARS

Ahmed A. Abouelfadl, Ioannis Psaromiligkos, Benoit Champagne

Department of Electrical and Computer Engineering, McGill University, Montreal, QC, Canada
ahmed.abouelfadl@mail.mcgill.ca, ioannis.psaromiligkos@mcgill.ca, benoit.champagne@mcgill.ca

ABSTRACT

A cognitive radar adapts its waveform to match the extended target's frequency response (TFR) for optimized detection performance. In practice, the TFR is unknown and is usually estimated using the Kalman filter assuming a linear Gaussian model. However, this assumption is not always fulfilled and other filters as the particle filter should be used. In all cases, existing approaches require the complete knowledge of the statistical distributions of both the TFR and interference. In this paper, we present a novel formulation of the TFR estimation problem that allows us to use the infinite hidden Markov model (iHMM) to estimate and track the TFR without such prior knowledge. Monte Carlo simulations considering Gaussian and non-Gaussian distributions for TFR and interference as well as jamming effects show that the proposed iHMM-based method ameliorates the estimation accuracy compared to the conventional Bayesian filtering techniques.

1. INTRODUCTION

Cognitive radar systems are distinguished by their dynamic adaptation of their transmitter and receiver operations through continuous learning from the environment [1, 2]. One goal of the transmitter adaptation is to optimize its waveform relative to the target of interest. An extended target can be viewed as a combination of multiple point targets and is modeled as a linear time-invariant or time-variant system and characterized by the target impulse response or, equivalently, by its target frequency response (TFR) [3, 4].

In practice, the TFR is unknown and is conventionally estimated as the hidden state of a state-space model using a Bayesian filter. For a linear Gaussian state-space model, a Bayesian filter is realized exactly by the Kalman filter (KF). For nonlinear Gaussian models, the KF can be approximated using extended, decoupled, unscented, or cubature KF [5]. If both the Gaussian and linear assumptions are not met, the particle filter (PF) is the best possible approximation for the Bayesian filter [6]. Previous works reported in the literature have focused on using the KF assuming Gaussian TFR and interference (noise and clutter) with known statistics [7–9], which are not always available.

In contrast to KF, the hidden Markov model (HMM) is not limited to linear Gaussian models. While in the KF the state transitions follow a continuous Gaussian linear model, the HMM assumes discrete states whose transitions follow a Markov chain. Interestingly, the discrete states assumption is well-suited to modern digital radar receivers, where the amplitudes of the processed signals are quantized to a finite number of values [10]. These observations motivate our investigation of applying the HMM to the TFR estimation problem. However, in a similar manner to KF and PF, to apply HMM to TFR estimation the model structure (e.g., transition probabilities) must be known, which is rarely the case. A promising solution to this difficulty is the nonparametric Bayesian framework, which when applied to the HMM results in the infinite HMM (iHMM).

In this paper, we provide a new formulation for the TFR estimation problem that makes it amenable to iHMM-based solutions. Then, we propose a new iHMM-based TFR estimation method that inherits all the desirable properties of nonparametric Bayesian approaches that is, it does not require any prior knowledge about the statistical properties of the TFR or the interference. Monte Carlo simulations are performed to compare the proposed method with the KF assuming Gaussian TFR and interference. We take the performance analysis a step further than the literature by considering the tracking performance over multiple pulses rather than the estimation performance at a single pulse. Moreover, we extend the analysis to the non-Gaussian TFR or clutter cases, for which we develop the PF and use it as a benchmark. Finally, we consider severe operating conditions such as smart noise jamming, which has not been considered before in TFR estimation context. Our simulations show that the proposed method outperforms KF and PF in terms of tracking error in all considered scenarios.

2. BACKGROUND: EXTENDED TARGET MODEL

Let $\tilde{\mathbf{g}} \in \mathbb{C}^{L_s}$ be the discrete-time transmitted radar waveform, which is fixed for M pulses, where L_s is the number of samples. A target with a range span larger than the radar's range cell can be divided into multiple, say L_t, discrete scattering centers. In this case, the total received signal at the mth pulse $\tilde{\mathbf{r}}^{(m)} \in \mathbb{C}^{L_s+L_t-1}$ is

$$\tilde{\mathbf{r}}^{(m)} = \tilde{\mathbf{g}} * \tilde{\mathbf{h}}^{(m)} + \tilde{\mathbf{c}}^{(m)} + \tilde{\mathbf{n}}^{(m)} \tag{1}$$

where * denotes convolution, $\tilde{\mathbf{h}}^{(m)} \in \mathbb{C}^{L_t}$ is the target impulse response, which changes on a pulse-to-pulse basis, $\tilde{\mathbf{c}}^{(m)}$ is the clutter vector and $\tilde{\mathbf{n}}^{(m)}$ is the noise vector. In this work, $\tilde{\mathbf{n}}^{(m)}$ and $\tilde{\mathbf{c}}^{(m)}$ are modeled as independent random vectors with $\tilde{\mathbf{n}}^{(m)} \sim \mathcal{CN}(\mathbf{0}, \mathbf{\Sigma}_n)$, while the distributions of $\tilde{\mathbf{h}}^{(m)}$ and $\tilde{\mathbf{c}}^{(m)}$ are discussed later.

After passing through an analog-to-digital converter (ADC), the baseband received signal $\tilde{\mathbf{r}}^{(m)}$ is passed through a receive filter of length L_s. The filter output of length $L_r = 2L_s + L_t - 2$ is then transformed to the frequency domain via an L_r-point discrete Fourier transform (DFT). Denoting $\mathfrak{T}\{\cdot\}$ as the combined effect of the L_r-point DFT and the receive filter operations, which are both linear, the frequency-domain received signal is

$$\mathbf{r}^{(m)} = \mathbf{G}\mathbf{h}^{(m)} + \mathbf{c}^{(m)} + \mathbf{n}^{(m)} \tag{2}$$

where $\mathbf{r}^{(m)} = \mathfrak{T}\{\tilde{\mathbf{r}}^{(m)}\}$, $\mathbf{G} = \text{diag}(\mathfrak{T}\{\tilde{\mathbf{g}}\})$ is the diagonal matrix of $\mathfrak{T}\{\tilde{\mathbf{g}}\}$, $\mathbf{h}^{(m)}$ is the target frequency response (TFR), $\mathbf{c}^{(m)} = \mathfrak{T}\{\tilde{\mathbf{c}}^{(m)}\}$, and $\mathbf{n}^{(m)} = \mathfrak{T}\{\tilde{\mathbf{n}}^{(m)}\}$.

978-1-7281-2723-1/19/$31.00 ©2019 IEEE

The TFR is usually assumed to be linear and Gaussian distributed, where the Bayesian filter for TFR estimation is realized using the KF. However, the conditions for the Gaussian assumption are not always met in real scenarios [11, 12]. Moreover, the clutter signals in many radar environments are non-Gaussian [13]. In such cases, the PF can be used [6], which is not limited to linear or Gaussian assumptions.

The lack of prior knowledge about the TFR distribution hinders the choice of the right approach for its estimation and tracking (over pulse index m) the TFR. Even if this information were available, knowledge of the distribution parameters would be necessary for the proper design of the Bayesian filter or any of its approximations. In this paper, we are concerned with estimating and tracking $\mathbf{h}^{(m)}$ from the received signal $\mathbf{r}^{(m)}$ without any prior information about $\mathbf{h}^{(m)}$ or interference terms $\mathbf{c}^{(m)}$ and $\mathbf{n}^{(m)}$.

3. TFR ESTIMATION AND TRACKING

In this section, we formulate of TFR estimation as a nonparametric Bayesian iHMM estimation problem and provide its solution.

3.1. TFR Modeling Using HMM

In related previous works, $\mathbf{h}^{(m)}$ is considered as a random vector with known distribution and generating model. This vector is estimated recursively over the pulse index m using a Bayesian filter [8]. Alternatively, we propose estimating $\mathbf{h}^{(m)} = [h_1^{(m)}, \cdots, h_l^{(m)}, \cdots, h_{L_r}^{(m)}]^T$, where $h_l^{(m)}$ denotes the lth frequency sample, by considering a recursion over the frequency index l within each pulse. The fact that the observations $\mathbf{r}^{(m)} = [r_1^{(m)}, , \cdots, r_l^{(m)} \cdots, r_{L_r}^{(m)}]^T$ are quantized to a finite number of quantization levels allows us to assume a discrete model for the amplitudes of the TFR samples. Regardless of the TFR generating model or distribution, the finite set of values taken by $h_l^{(m)}$ can be seen as the possible states in a scalar stochastic finite state machine (SFSM). In the SFSM, the sample amplitude at frequency l can transit from a given state to any other state at frequency $l+1$ according to a certain probability distribution. Specifically, the TFR samples for each pulse can be modeled as an HMM, a type of SFSM in which the output value (i.e. $r_l^{(m)}$) associated to each state is also stochastic and the states are hidden from the observer [14].

To apply the HMM to the TFR at the mth pulse, the components of $\mathbf{h}^{(m)}$ are considered as the hidden state sequence, while the components of $\mathbf{r}^{(m)}$ are the observations. Each sample of $\mathbf{h}^{(m)}$ or $\mathbf{r}^{(m)}$ can take any value from the discrete level sets, $\mathbf{Q} = \{q_1, \cdots, q_{N_s}\}$ or $\mathbf{O} = \{o_1, \cdots, o_{N_o}\}$, respectively. Without loss of generality, it is assumed that $N_s = N_o \equiv N$, where N denotes the quantization levels of the used ADC. Within the mth pulse, we assume that the components of $\mathbf{h}^{(m)}$ form a Markov chain of first order, that is

$$\Pr(h_l^{(m)} = q_i | h_{l-1}^{(m)} = q_j, \cdots, h_1^{(m)} = q_k) = \Pr(h_l^{(m)} = q_i | h_{l-1}^{(m)} = q_k) \quad (3)$$

where $1 \le i, j, k \le N$ and $1 \le l \le L_R$. We also assume a homogeneous HMM within the same pulse, but not from pulse to pulse. That is, the probabilities in (3) do not depend on l but may change with m. To simplify the notation, we temporarily drop the index m noting that the following steps are applied to each pulse.

To estimate the hidden states, the HMM structure should be specified *a priori*. For $1 \le l \le L_r$, this structure is defined by: *(1)* the discrete sets of states $\mathbf{Q}$ and observations $\mathbf{O}$; *(2)* the state transition matrix $\mathbf{A} = [a_{ij}] = \Pr(h_l = q_j | h_{l-1} = q_i)$, $1 \le i, j \le N$; *(3)* the emission matrix $\mathbf{B} = [b_{ij}] = \Pr(r_l = o_j | h_l = q_i)$, $1 \le i, j \le N$. Both $\mathbf{A}$ and $\mathbf{B}$ do not depend on l based on the homogeneity assumption. To achieve both low quantization noise and high dynamic range, the number of bits of the ADC can be as high as 14 bits or more [15]. This implies transition and emission matrices of very high dimensions, let alone the difficulty of obtaining prior knowledge about them.

3.2. Employing iHMM in TFR Modeling

Inspired by the nonparametric Bayesian models, the problem of determining $\mathbf{A}$ and $\mathbf{B}$ can be avoided using an iHMM with unbounded number of states [16]. In iHMM, only a finite number of states, say K, are invoked initially at $m = 1$; K may grow or shrink for $m > 1$ depending on $\mathbf{r}^{(m)}$. Each row of $\mathbf{A}$ or $\mathbf{B}$ is modeled using a Dirichlet process (DP), also known as stick-breaking process, with possibly unbounded number of components (in our case $K \le N$). As both $\mathbf{r}$ and $\mathbf{h}$ are for the same target, the DP of the rows of $\mathbf{A}$ as well as those of the rows of $\mathbf{B}$ should be linked. To model this relationship, we propose using the hierarchical DP (HDP) [17].

For any $\gamma > 0$, we define the infinite length random vector $\boldsymbol{\beta} = [\beta_i]_{i=1}^{\infty} \triangleq \text{Stick}(\gamma)$ as [17]

$$\beta_i = \hat{\beta}_i \Pi_{k=1}^{i-1}(1 - \hat{\beta}_k), \qquad \hat{\beta}_k \overset{iid}{\sim} \text{Beta}(1, \gamma) \quad (4)$$

where $\text{Beta}(1, \gamma)$ denotes the Beta distribution with shape parameters 1 and γ. The ith row of $\mathbf{A}$ of length K is

$$\mathbf{a}_i = [a_{ij}, \cdots, a_{iK}] \sim \text{Dir}(\alpha\beta_1, \cdots, \alpha\beta_K) \quad (5)$$

where Dir denotes the Dirichlet distribution and α is a non-negative scalar. The emission matrix $\mathbf{B}$ is generated in the same way as in (4) and (5), but using $\boldsymbol{\beta}^e$, γ^e, and α^e. Therefore, using HDP, the rows of $\mathbf{A}$ are linked through the common vector $\boldsymbol{\beta}$. Similarly, the rows of $\mathbf{B}$ are linked through the common vector $\boldsymbol{\beta}^e$. Hence, using only four hyperparameters $\alpha, \alpha^e, \gamma, \gamma^e$, the iHMM model is fully specified and controlled.

3.3. TFR Estimation Using iHMM

In the following, we show how to infer the state sequence $\mathbf{h}$ and the iHMM hyperparameters for each pulse. The first step in estimating $\mathbf{h}$ is to estimate the posterior probability density function (pdf) $f(h_l | r_{1:l})$ of the lth sample within the L_r samples, where $r_{1:l} = [r_1, \cdots, r_l]$. The canonical state inference algorithm is the Gibbs sampler, however, its convergence is slow, especially with correlated data. Moreover, the posterior and the prior pdfs of $\mathbf{h}$ should be conjugate. To avoid these drawbacks, we adopt another inference algorithm, the beam sampling [18].

The beam sampler utilizes auxiliary variables to reduce the states of $\mathbf{A}$ and $\mathbf{B}$ at each l resulting in a finite number of states. Consequently, dynamic programming algorithms can be used to estimate the posterior pdf of the states as in the conventional HMM. Using the auxiliary variables $u_{1:L_r} = [u_1, \cdots, u_{L_r}]$, the posterior pdf can be estimated as [18]

$$f(h_l | r_{1:L_r}, u_{1:L_r}) \propto f(r_l | h_l) \sum_{u_l < \Pr(h_l | h_{l-1})} f(h_{l-1} | r_{1:l-1}, u_{1:l-1}) \quad (6)$$

In (6), the sum at each l is evaluated only over a limited number of states, say K_u, out of the invoked states K, whose transition

probabilities exceed a threshold u_l. The choice of u_l is important. On one hand, a large u_l may result in underestimating the actual number of states. On the other hand, a small u_l may result in a higher number of states that increases the complexity of the model and the resulting error. The threshold is conventionally taken as $u_l \sim \mathcal{U}(0, \Pr(h_{L_r}|h_{l-1}))$ with $\mathcal{U}(a,b)$ denoting the uniform distribution in the interval $[a,b]$ [16], or $u_l \sim \Pr(h_{L_r}|h_{l-1})\text{Beta}(w,z)$ with $w,z>0$ [19]. In the latter case, the appropriate choices of w and z, which have not been specified in the literature, should force u_l to be either close to 0 or $\Pr(h_{L_r}|h_{l-1})$. In this work, we propose adjusting u_l depending on the pulse number m. Since there is no prior information about the true states of $\mathbf{h}^{(m)}$, the model is initialized at $m=0$ with a low K. As m advances, the number of the invoked states K grows and, consequently, their relative transition probabilities tends to be lower. Therefore, u_l needs to be decreased as m increases, otherwise the number of surviving states K_u will be too low for an accurate estimation of $\mathbf{h}^{(m)}$. The details of the choice iHMM parameters are provided in Section 4.

Finally, to estimate the state sequence $\mathbf{h}$, h_{L_r} is first sampled using $f(h_{L_r}|r_{1:L_r}, u_{1:L_r})$, then the backward induction is used to estimate the remaining states from the posterior pdf as [18]

$$f(h_l|h_{l+1}, r_{1:L_r}, u_{1:L_r}) \propto f(h_{l+1}|h_l, u_{l+1}) f(h_l|r_{1:l}, u_{1:l}) \quad (7)$$

The process of estimating $\mathbf{h}^{(m)}$ is performed for each received signal $\mathbf{r}^{(m)}$, where the hyperparameters inferred based on $\mathbf{h}^{(m-1)}$ are used in generating $\mathbf{A}$ and $\mathbf{B}$ to estimate $\mathbf{h}^{(m)}$.

After inferring the states, we infer the model hyperparameters α, γ, α^e, and γ^e as a second step. For $\mathbf{A}$, at $m=0$ the two hyperparameters α and γ are initialized as [18]

$$\alpha^{(0)} \sim \text{Gamma}(a_\alpha, b_\alpha), \qquad \gamma^{(0)} \sim \text{Gamma}(a_\gamma, b_\gamma), \quad (8)$$

where $\text{Gamma}(a,b)$ denotes the Gamma distribution with shape parameter a and inverse scale parameter b, where $a_\alpha, b_\alpha, a_\gamma, b_\gamma > 0$. At the mth pulse, $\alpha^{(m)}$ is generated as [20, eq. (47)]

$$\alpha^{(m)} \sim \text{Gamma}(a_\alpha + E - \sum_{k=1}^{K_u} e_k, b_\alpha - \sum_{k=1}^{K_u} \log q_k), \quad (9)$$

where e_k is a binary variable that randomly takes a value of 0 or 1, E is the number of inferred states within $\mathbf{h}^{(m)}$ obtained after solving the dynamic program in the TFR inference step, and $q_k \sim \text{Beta}(\alpha^{(m-1)}+1, n)$ with n being the number of times each state of E is visited. Moreover, $\gamma^{(m)}$ is obtained by [17, eq. (13)]

$$\begin{aligned}\gamma^{(m)} \sim & \pi_\eta \text{Gamma}(a_\gamma + E, b_\gamma - \log(\eta)) + \\ & (1-\pi_\eta)\text{Gamma}(a_\gamma + E - 1, b_\gamma - \log(\eta))\end{aligned} \quad (10)$$

where $\pi_\eta = (a_\gamma + E - 1)/(E(b_\gamma - \log(\eta)))$ and $\eta \sim \text{Beta}(\gamma^{(m-1)}+1, E)$. Equations (8), (9) and (10) can be applied to infer α^e, γ^e given h_l using $a_{\alpha^e}, b_{\gamma^e}$ as initialization parameters, K_u^e as the number of surviving output values, n^e as the number of times an output value is visited, and E^e as the total number of visited observations.

4. PERFORMANCE EVALUATION

In this section we evaluate the TFR estimation accuracy of the proposed iHMM-based method and compare it to the particle and KF through Monte Carlo simulations.

4.1. Simulation Setup

The radar transmitted waveform $\tilde{\mathbf{g}}$ is simulated as a linear frequency modulated signal with 1 MHz bandwidth and 4 μs pulse width sampled at 2.5 MHz and the ADC has $N = 2^{14}$ quantization levels. The TFR is modeled as a state-space model $\mathbf{h}^{(m)} = e^{-T_r/\zeta}\mathbf{h}^{(m-1)} + \mathbf{v}^{(m-1)}$ [8], where ζ is the decay time constant, T_r is the radar pulse repetition interval, and $\mathbf{v}^{(m-1)}$ is the white Gaussian state noise vector in frequency domain. Both $\mathbf{v}^{(m-1)}$ and $\mathbf{h}^{(m-1)}$ are assumed to be independent. While the iHMM is not limited to a linear state-space model, we adhere to it in this paper to compare the proposed method with the literature [8, 9]. The TFR is initialized as a Gaussian or non-Gaussian vector, with $L_t = 4$ and $T_r/\zeta = 0.001$. The non-Gaussian $\tilde{\mathbf{h}}^{(m)}$ is represented by a $K-$distributed vector generated from a spherical invariant random process [21, 22]. In both cases, $\tilde{\mathbf{h}}^{(m)}$ has a zero mean and covariance matrix $\mathbf{\Sigma}_h = \mathbf{I}$, where $\mathbf{I}$ is the $L_t \times L_t$ identity matrix. The clutter vector $\tilde{\mathbf{c}}$ is generated in the same way as $\mathbf{h}$ for both Gaussian and K-distributions with a covariance matrix $\mathbf{\Sigma}_c = [0.9^{|i-j|}], 1 \le i,j \le L_s$.

The estimation error is calculated over $M = 16$ pulses using the normalized root mean square error (NRMSE) defined as

$$\epsilon(m) = \|\mathbf{h}^{(m)} - \hat{\mathbf{h}}^{(m)}\|_2 / \|\bar{\mathbf{h}}\|_2 \quad (11)$$

where $\mathbf{h}^{(m)}$ and $\hat{\mathbf{h}}^{(m)}$ are the true and estimated TFR at the mth pulse, respectively, $\bar{\mathbf{h}}$ is the sample mean of the true TFR over the 16 pulses, and $\|\cdot\|_2$ denotes the ℓ_2-norm. The NRMSE is averaged over 250 trials.

The performance of the proposed method is compared to the KF in the case of Gaussian $\mathbf{h}^{(m)}$ and $\mathbf{c}^{(m)}$. The minimum mean square error (MMSE) estimator is used to initialize the KF and the final estimate is taken after 50 iterations. In the case of K-distributed $\mathbf{h}^{(m)}$ and/or $\mathbf{c}^{(m)}$, we apply the PF with $N_p = 50$ particles, with the ith particle at the m-th pulse having a weight $w_i^{(m)}$ calculated as [23, eq. (63)]

$$w_i^{(m)} \propto w_i^{(m-1)} f(\mathbf{r}^{(m)}|\mathbf{h}^{(m)}) \qquad i = 1, \cdots, N_p \quad (12)$$

where $f(\mathbf{r}^{(m)}|\mathbf{h}^{(m)})$ is the likelihood pdf of $\mathbf{r}^{(m)}$, which is as deduced for the K- distributed clutter in [24]. To overcome the degeneracy problem, the particles with negligible weights are removed and N_p particles are resampled, each with a weight $1/N_p$ [23].

In the iHMM, we found through simulations that $u_l = 10^{-\kappa}\mathcal{U}(0, \Pr(h_t|h_{t-1}))$, with $\kappa = 0.15m$, is an appropriate value. There are no recommended values for a_α, a_γ and b_α, b_γ in the literature, but we found $a_\alpha, a_\gamma \sim \mathcal{U}(1,10)$ and $b_\alpha, b_\gamma \sim \mathcal{U}(0.1,1)$ to be appropriate. Again, these choices are independent on the distribution of $\mathbf{h}^{(m)}$ or $\mathbf{c}^{(m)}$. For the PF and KF, we assume three scenarios. In the first scenario the filters have perfect prior knowledge about the statistics parameters of $\mathbf{h}^{(m)}$, $\mathbf{c}^{(m)}$, and $\mathbf{n}^{(m)}$. The second case assumes partial knowledge of the latter three vectors, that is, the distributions are known, but not their parameters. In the third case, the filters have no prior knowledge about the three vectors.

4.2. Results and Discussion

Assuming Gaussian $\mathbf{h}^{(m)}$, $\mathbf{c}^{(m)}$ and linear $\mathbf{h}^{(m)}$ model, the KF can be used to estimate $\mathbf{h}^{(m)}$. Fig. 1 shows that the KF provides the lowest error at $m=1$ compared to the PF and iHMM. However, beyond $m=1$, its error is proportional to m at a higher rate than that of the PF and above the iHMM. This lower error is ascribed to the fact that the KF is the exact Bayesian filter for the TFR estimation problem under the assumption of Gaussian $\mathbf{h}^{(m)}$ and $\mathbf{c}^{(m)}$. Nevertheless, as

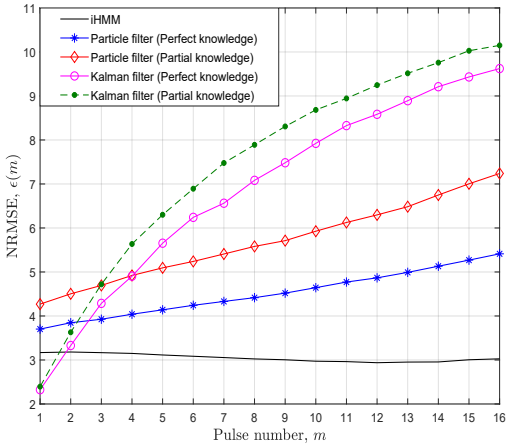

Fig. 1. Estimation error of Gaussian TFR in Gaussian clutter.

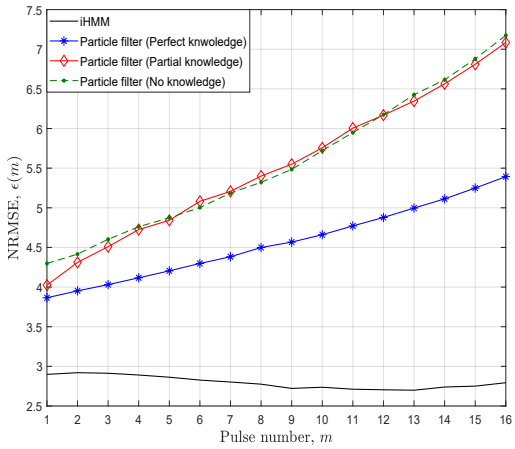

Fig. 3. Estimation error of $K-$distributed TFR and clutter.

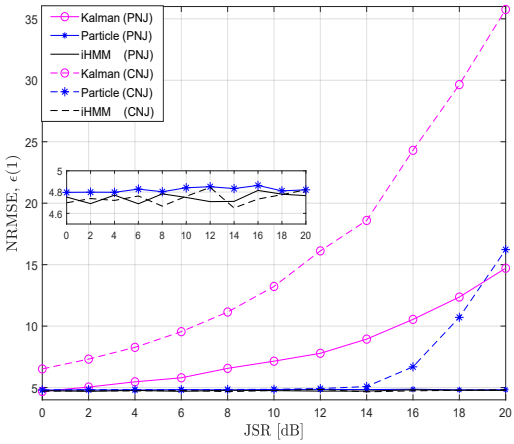

Fig. 2. Estimation error of Gaussian TFR in jamming and Gaussian clutter ($m = 1$).

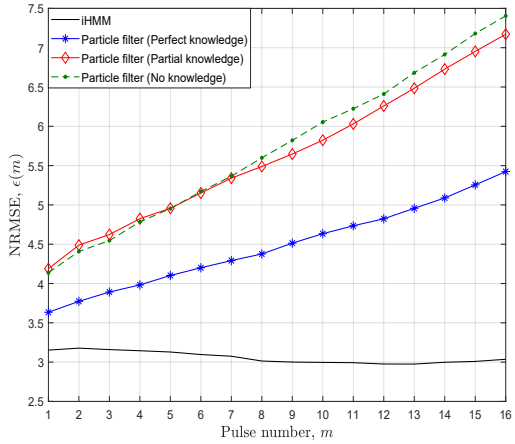

Fig. 4. Estimation error of Gaussian TFR in $K-$distributed clutter.

$\mathbf{h}^{(m)}$ itself is a random vector, the model mismatch increases with the accumulation of noise as m increases.

However, even this relative lower error of the KF at $m = 1$ is not guaranteed in all operating conditions. Specifically, when the radar system is under the effect of jamming. We use the pulsed noise jamming (PNJ) and the convolution noise jamming (CNJ) to evaluate the performance of the three methods. Both are generated by a repeater jammer matched to the radar pulse width and repetition interval [25]. CNJ is the result of the convolution between the intercepted radar pulse and a noise pulse generated by the jammer. Fig. 2 shows ϵ at $m = 1$ under the effect of the PNJ and CNJ versus different jamming-to-signal ratios (JSRs). Compared to the jamming-free case, the KF is vulnerable to both jamming techniques, especially to the CNJ, with a higher ϵ that increases with the (JSR). For the PF, ϵ is higher at all JSR values in the case of PNJ, while ϵ increases significantly at higher JSRs under the effect of the CNJ. Except for the small increase in ϵ at all JSRs, the iHMM shows better stability in terms of ϵ in the presence of both PNJ and CNG.

Fig. 3 shows ϵ of the $K-$distributed $\mathbf{h}^{(m)}$ and $\mathbf{c}^{(m)}$ for both the iHMM and PF. Even when the PF has perfect knowledge about both $\mathbf{h}^{(m)}$ and $\mathbf{c}^{(m)}$, ϵ increases with m. If this perfect knowledge is not provided, ϵ is higher and increases in a faster rate. This is true whether the PF has prior partial knowledge or it has no information about $\mathbf{h}^{(m)}$ and $\mathbf{c}^{(m)}$. On the contrary, the iHMM shows a lower ϵ at pulses and it does not increase with m; it even slightly decreases. Fig. 4 shows the performance for the Gaussian $\mathbf{h}^{(m)}$ with $K-$distributed $\mathbf{c}^{(m)}$. It is observed that the iHMM shows the same error trend as for the $K-$distributed $\mathbf{h}^{(m)}$, but with a slight increase in ϵ at all m. While the PF introduces a lower ϵ at $m = 1$ relative to its error with the $K-$distributed $\mathbf{h}^{(m)}$, it reaches approximately the same error at the $m = 16$ for the three cases considered.

5. CONCLUSION

In this paper we delved into the problem of Gaussian and non-Gaussian TFR estimation under the assumption of Gaussian and non-Gaussian clutter. In this context, the performance of the non-parametric Bayesian framework represented by the iHMM is compared to the classic Bayesian frameworks of the KF and PF. Compared to the latter filters, the iHMM improves the tracking accuracy of the TFR without any prior knowledge about its statistics or that of the interference, even if the filters know perfectly the statistical parameters of the TFR and interference. These promising results encourage further research in employing the nonparametric Bayesian methods in cognitive radar applications.

6. REFERENCES

[1] S. Haykin, "Cognitive radar: a way of the future," *IEEE Signal Process. Mag.*, vol. 23, pp. 30–40, Jan. 2006.

[2] M. S. Greco, F. Gini, P. Stinco, and K. Bell, "Cognitive radars: On the road to reality: Progress thus far and possibilities for the future," *IEEE Signal Process. Mag.*, vol. 35, pp. 112–125, July 2018.

[3] M. Richards, W. Holm, W. Melvin, J. Scheer, and J. Scheer, *Principles of Modern Radar: Basic Principles*. North Carolina: Institution of Engineering and Technology, 2012.

[4] H. L. V. Trees, *Detection, Estimation, and Modulation Theory: Radar-Sonar Signal Processing and Gaussian Signals in Noise*. Melbourne, FL, USA: Krieger Publishing Co., Inc., 1992.

[5] S. Haykin, Y. Xue, and P. Setoodeh, "Cognitive radar: Step toward bridging the gap between neuroscience and engineering," *Proc. IEEE*, vol. 100, pp. 3102–3130, Nov. 2012.

[6] S. Haykin, *Cognitive Dynamic Systems: Perception-action Cycle, Radar and Radio*. Cambridge University Press, 2012.

[7] P. Chen and L. Wu, "Waveform design for multiple extended targets in temporally correlated cognitive radar system," *IET Radar, Sonar Navigation*, vol. 10, pp. 398–410, Feb. 2016.

[8] X. Zhang, K. Wang, and X. Liu, "Joint optimisation of transmit waveform and receive filter for cognitive radar," *IET Radar, Sonar Navigation*, vol. 12, pp. 11–20, Jan. 2018.

[9] B. Tang, J. Tang, and Y. Peng, "MIMO radar waveform design in colored noise based on information theory," *IEEE Trans. Signal Process.*, vol. 58, pp. 4684–4697, Sep. 2010.

[10] D. C. Jenn, P. E. Pace, and R. A. Romero, "An antenna for a mast-mounted low probability of intercept continuous wave radar: Improving performance with digital architecture," *IEEE Antennas Propag. Mag.*, vol. 61, pp. 63–70, April 2019.

[11] A. De Maio, A. Farina, and G. Foglia, "Target fluctuation models and their application to radar performance prediction," *IEE Proceedings - Radar, Sonar and Navigation*, vol. 151, pp. 261–269, Oct. 2004.

[12] G. A. Clark, "Non-Gaussian correlated process sampling for Bayesian cognitive target classification," *The J. of the Acoustical Society of America*, vol. 137, 2015.

[13] A. Mezache, F. Soltani, M. Sahed, and I. Chalabi, "Model for non-Rayleigh clutter amplitudes using compound inverse Gaussian distribution: an experimental analysis," *IEEE Trans. Aerosp. Electron. Syst.*, vol. 51, pp. 142–153, Jan. 2015.

[14] H. Bourlard and S. Bengio, "Hidden Markov models and other finite state automata for sequence processing," tech. rep., IDIAP, 2001.

[15] S. Turso and T. Bertuch, "Zero-IF radar signal processing," in *European Radar Conf. (EuRAD)*, pp. 513–516, Sep. 2015.

[16] M. J. Beal, Z. Ghahramani, and C. E. Rasmussen, "The infinite hidden Markov model," in *Proc. of the 14th Int. Conf. on Neural Information Processing Systems: Natural and Synthetic*, NIPS'01, (Cambridge, MA, USA), pp. 577–584, MIT Press, 2001.

[17] M. D. Escobar and M. West, "Bayesian density estimation and inference using mixtures," *J. Am. Stat. Assoc.*, vol. 90, no. 430, pp. 577–588, 1995.

[18] J. Van Gael, Y. Saatci, Y. W. Teh, and Z. Ghahramani, "Beam sampling for the infinite hidden Markov model," in *Proc.of the International Conf. on Machine Learning*, pp. 1088–1095, ACM, 2008.

[19] J. V. Gael and Z. Ghahramani, "Nonparametric hidden Markov models," in *Bayesian Time Series Models* (D. Barber, A. T. Cemgil, and S. Chiappa, eds.), p. 317340, Cambridge University Press, 2011.

[20] Y. W. Teh, M. I. Jordan, M. J. Beal, and D. M. Blei, "Hierarchical Dirichlet processes," *J. Am. Stat. Assoc.*, vol. 101, no. 476, pp. 1566–1581, 2006.

[21] Ahmed A. Abouelfadl, I. Psaromiligkos, and B. Champagne, "Covariance-free nonhomogeneity STAP detector in compound Gaussian clutter based on robust statistics," *IET Radar, Sonar & Navigation*, to be published.

[22] Ahmed A. Abouelfadl, I. Psaromiligkos, and B. Champagne, "A low-complexity nonparametric STAP detector," in *IEEE National Aerospace and Electronics Conf. (NAECON)*, (Ohio, USA), pp. 592–596, July 2018.

[23] M. S. Arulampalam, S. Maskell, N. Gordon, and T. Clapp, "A tutorial on particle filters for online nonlinear/non-Gaussian Bayesian tracking," *IEEE Trans. Signal Process.*, vol. 50, pp. 174–188, Feb. 2002.

[24] A. Farina and P. Lombardo, "Modelling of a mixture of K-distributed and Gaussian clutter for coherent radar detection," *Electron. Lett.*, vol. 30, pp. 520–521, March 1994.

[25] Ahmed A. Abouelfadl, A. M. Samir, F. M. Ahmed, and A. H. Asseesy, "Performance analysis of LFM pulse compression radar under effect of convolution noise jamming," in *National Radio Science Conf. (NRSC)*, (Aswan, Egypt), pp. 282–289, Feb. 2016.